Acta Crystallographica Section D
Biological Crystallography
ISSN 0907-4449

Structure of the catalytic nucleotide-binding subunit A of A-type ATP synthase from *Pyrococcus horikoshii* reveals a novel domain related to the peripheral stalk

Yuki Maegawa, Hazuki Morita, Daisuke Iyaguchi, Min Yao, Nobuhisa Watanabe* and Isao Tanaka

Division of Biological Sciences, Graduate School of Science, Hokkaido University, Japan

Correspondence e-mail: nobuhisa@sci.hokudai.ac.jp

Received 21 December 2005
Accepted 20 February 2006

PDB Reference: A_1-ATPase A subunit, 1vdz, r1vdzsf.

H^+-transporting ATP synthase is a multi-subunit enzyme involved in the production of ATP, which is an essential molecule for living organisms as a source of energy. Archaeal A-type ATPase (A-ATPase) is thought to act as a functional ATP synthase in archaea and is thought to have chimeric properties of F-ATPase and V-ATPase. Previous structural studies of F-ATPase indicated that the major nucleotide-binding subunits α and β consist of three domains. The catalytic nucleotide-binding subunit A of V/A-ATPase contains an insertion of about 90 residues which is absent from the F_1-ATPase β subunit. Here, the first X-ray structure of the catalytic nucleotide-binding subunit A of an A_1-ATPase is described, determined at 2.55 Å resolution. A_1-ATPase subunit A from *Pyrococcus horikoshii* consists of four domains. A novel domain, including part of the insertion, corresponds to the 'knob-like structure' observed in electron microscopy of A_1-ATPase. Based on the structure, it is highly likely that this inserted domain is related to the peripheral stalk common to the A- and V-ATPases. The arrangement of this inserted domain suggests that this region plays an important role in A-ATPase as well as in V-ATPase.

1. Introduction

H^+-transporting ATP synthase (H^+-ATPase; EC 3.6.3.14) is a multi-subunit enzyme involved in the production of ATP. F-type ATPase (F-ATPase) acts as a functional ATP synthase in rotational mode driven by a proton electrochemical potential gradient (Yasuda *et al.*, 2001). The vacuolar-type ATPase in vacuoles and clathrin-coated vesicles (V-ATPase) pumps H^+ rather than synthesizing ATP under physiological conditions, although its structure is similar to that of the F-type enzyme (Forgac, 1999; Futai *et al.*, 1998). Archaeal A-type ATPase (A-ATPase) is the third class belonging to the H^+-translocating ATPase superfamily (Schafer & Meyering-Vos, 1992) and is thought to have chimeric properties of F-ATPase and V-ATPase with regard to structure and function (Becher & Muller, 1994; Mukohata & Yoshida, 1987; Ihara & Mukohata, 1991; Hochstein, 1992; Dirmeier *et al.*, 2000; Wilms *et al.*, 1996). Each enzyme in the three classes mentioned above consists of two sectors: a hydrophilic catalytic headpiece sector ($F_1/V_1/A_1$) and a membrane sector ($F_0/V_0/A_0$) (Fig. 1*a*). The catalytic headpiece sectors (containing the $\alpha_3\beta_3$ subcomplex in F_1 and A_3B_3 in V_1/A_1) are connected to the membrane sectors *via* the F_1-ATPase γ subunit or the V_1/A_1-ATPase D subunit. The major nucleotide-binding subunits in F_1-ATPase are the catalytic β and non-catalytic α subunits, whereas the corresponding subunits in V_1/A_1-ATPase are the catalytic A and non-

catalytic B subunits. Previous structural studies have indicated that F_1 α and β subunits consist of three domains: the N-terminal domain, the nucleotide-binding domain and the C-terminal domain (Abrahams *et al.*, 1994; Leyva *et al.*, 2003). However, the catalytic subunit A of V_1/A_1 contains an insertion of about 90 residues called the non-homologous region (NHR) between the N-terminal and nucleotide-binding domains (Zimniak *et al.*, 1988; Bowman *et al.*, 1988; Hirata *et*

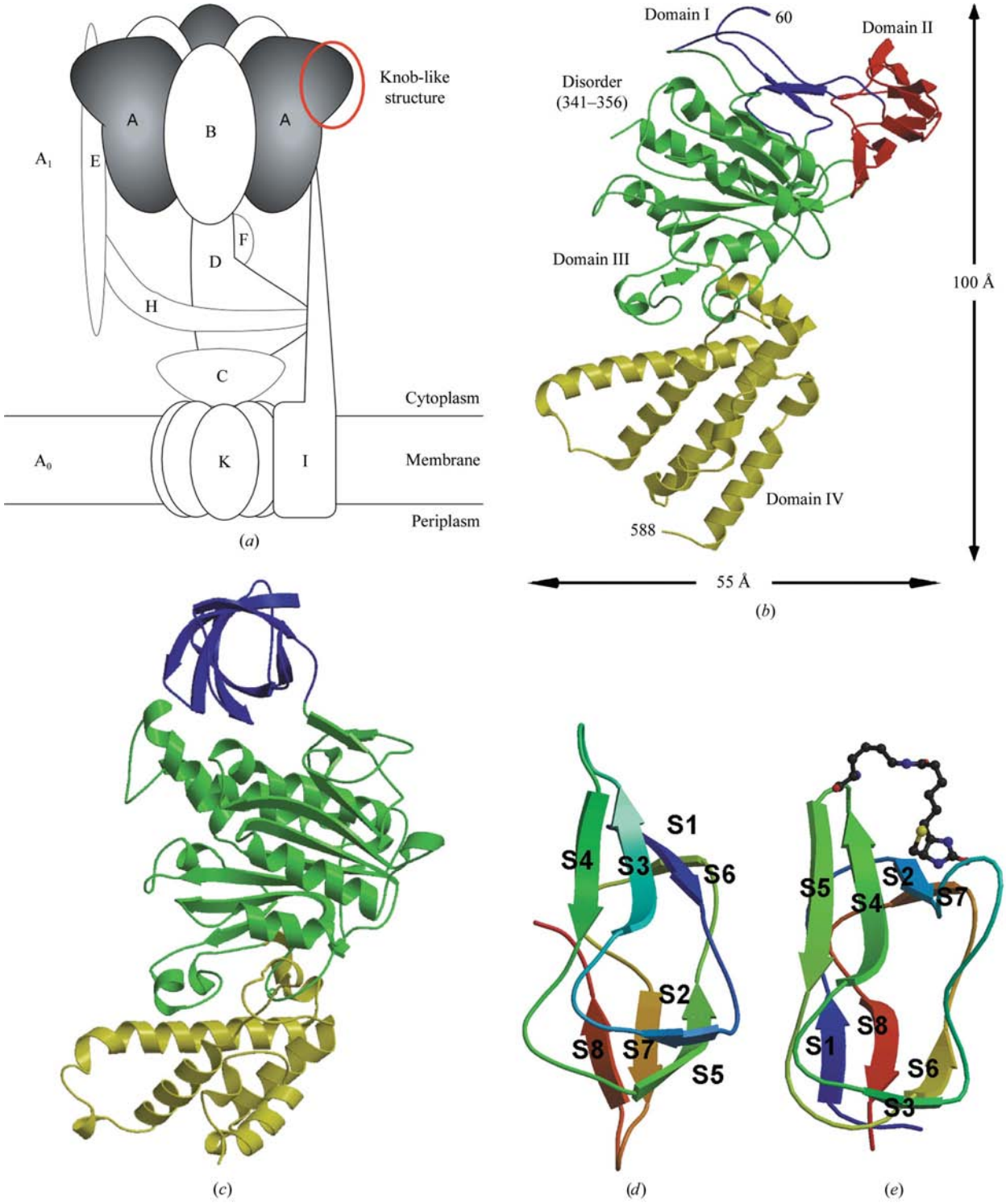

Figure 1
Catalytic nucleotide-binding subunit A of *Pho* A-ATPase. (*a*) Schematic model based on the model of *Methanococcus janashii* A-ATPase (Coskun, Chaban *et al.*, 2004). Three catalytic A subunits are coloured grey. (*b*) Structure of *Pho* A-ATPase catalytic nucleotide-binding subunit A. (*c*) Overall structure of the catalytic nucleotide-binding subunit β of bovine mitochondrial F-ATPase (empty form). (*d*) Domain II. The direction of view is approximately horizontal to that in (*b*). Eight β-strands are labelled S1–S8, respectively. (*e*) Archetype of the similar structures of domain II and the biotinyl domain of acetyl-CoA carboxylase (PDB code 1bdo). The biotinylated lysine residue is represented as a ball-and-stick model.

al., 1990; Puopolo *et al.*, 1991) which is highly conserved among A subunits but is absent from the F_1 β subunit. The results of mutational analysis of this region of the *Saccharomyces cerevisiae* (*Sce*) V_1 A subunit suggested that the NHR is likely to form a unique domain and to form part of a peripheral stalk connection between the V_1 and V_0 domains (Shao *et al.*, 2003; Shao & Forgac, 2004). Moreover, recently reported structures of the A_1 headpiece and of A_1A_0 obtained by electron microscopy revealed the existence of a knob-like structure in the catalytic subunit A which is not found in the F_1 headpiece (Coskun, Radermacher *et al.*, 2004; Coskun, Chaban *et al.*, 2004).

Here, we report the first X-ray structure of the catalytic nucleotide-binding subunit A of A_1-ATPase at 2.55 Å resolution.

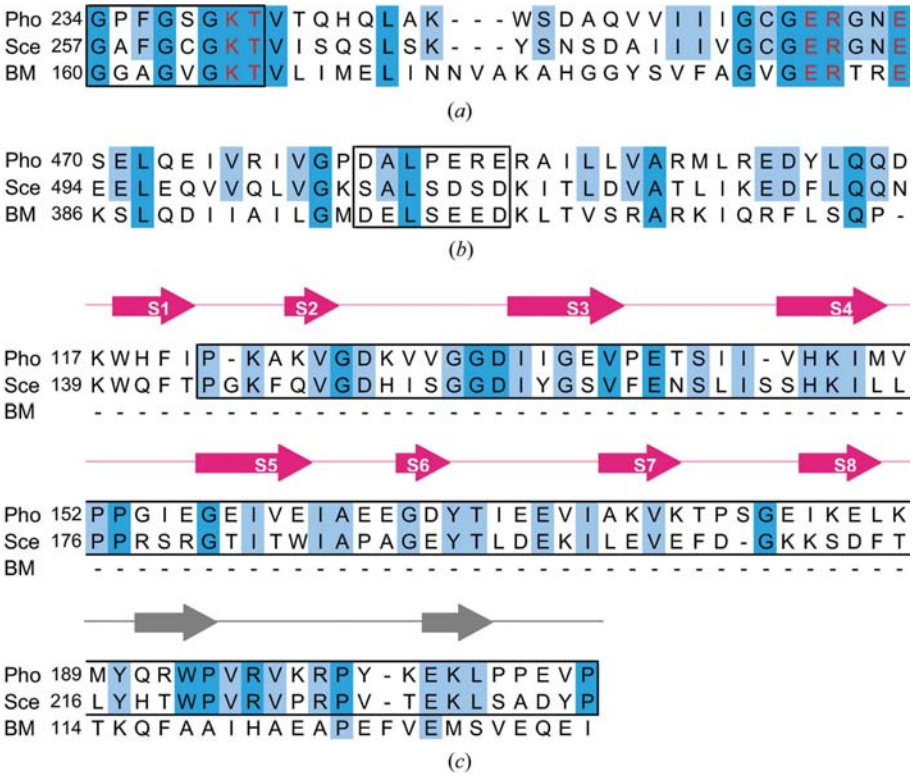

Figure 2
Amino-acid sequence comparison of A/V/F-ATPase catalytic nucleotide-binding subunits. Pho, *Pho* A-ATPase$_1$ A subunit; Sce, *Sce* V_1-ATPase A subunit; BM, bovine mitochondrial F_1-ATPase β subunit. (*a*) The nucleotide-binding site. Only residues corresponding to Gly234–Glu267 in the *Pho* A_1-ATPase A subunit are shown. Residues conserved in the catalytic nucleotide-binding subunits are shown in blue. Residues identical in Pho and Sce are shown in light blue. The sequence highlighted in the box corresponds to the nucleotide-binding P-loop. Nucleotide-binding residues are shown in red. (*b*) Comparison around the DALPERE sequence (residues 482–488) corresponding to DELSEED in F_1-ATPase β. Residues conserved in the catalytic nucleotide-binding subunits are shown in blue. Residues identical in Pho and Sce are shown in light blue. The sequence highlighted in the box corresponds to the F_1-ATPase β DELSEED region. (*c*) Domain II (coloured pink above the sequences) and the previously assigned NHR (Pro122–Pro210 of the *Pho* A_1 A subunit, highlighted in the box). Only residues corresponding to Lys117–Pro210 in the *Pho* A_1-ATPase A subunit are shown. Met189–Pro210 of the *Pho* A_1-ATPase A subunit and Thr114–Ile136 of the bovine F_1 β subunit are homologous (coloured grey). Residues identical in all known sequences of A_1-ATPase and V_1-ATPase A subunits are shown in blue. Residues identical in Pho and Sce are shown in light blue. Secondary-structure elements including eight β-strands of Pho domain II (pink arrows labelled S1–S8) and two β-strands conserved in Pho and BM (grey arrows) are indicated above the sequences.

2. Materials and methods

2.1. Crystallization and data collection

Pyrococcus horikoshii (*Pho*) ATPase subunit A was expressed, purified and crystallized in a form corresponding to the product of intein-mediated protein splicing as described previously (Maegawa *et al.*, 2004). Crystals of selenomethionine (SeMet) substituted A subunit were also prepared for MAD phasing. In the case of SeMet-substituted A subunit, cells were grown at 310 K in M9 minimal medium supplemented with 25 µg ml^{-1} SeMet in place of methionine, 50 µg ml^{-1} ampicillin and thiamine. At an OD_{600} of 0.6, the cells were induced by addition of 1 m*M* IPTG and growth continued at 310 K for 17 h. Subsequent steps were the same as described for the native protein and crystals of the SeMet-substituted A subunit were obtained under the same conditions (Maegawa *et al.*, 2004).

All X-ray diffraction experiments were performed at 100 K with crystals cooled in a nitrogen-gas stream. Crystallization solution [46–50%(*v*/*v*) MPD] was also used as cryoprotectant solution. The native data set was collected at beamline BL41XU of SPring-8 and a complete MAD data set from a single crystal of SeMet-incorporated A subunit was collected at beamline BL18B of Photon Factory. Data-collection statistics are summarized in Table 1.

2.2. Structure determination and crystallographic refinement

11 of the 18 expected Se sites in the asymmetric unit were found by *SOLVE* (Terwilliger, 2004) and were further refined using *SHARP* (de La Fortelle & Bricogne, 1997). Finally, 17 Se sites were found and used to phase the structure factor with *SHARP*. The electron densities were improved by solvent flattening with *SOLOMON* (Abrahams & Leslie, 1996). Density modification was performed with *ARP*/*wARP* (Morris *et al.*, 2003) and *DM* (Cowtan, 1994) from the *CCP*4 program package (Collaborative Computational Project, Number 4, 1994). The initial model of subunit A was built manually using the program *O* (Jones *et al.*, 1991). Crystal averaging between the native and SeMet crystals using *DMMULTI* (Cowtan, 1994) from the *CCP*4 program package (Collaborative Computational Project,

Table 1
Crystallographic statistics.

Values in parentheses are for the outermost resolution shell.

		SeMet derivative		
	Native	Peak	Edge	Remote
X-ray data				
Wavelength	0.9000	0.9795	0.9797	0.9600
Space group	$P4_32_12$			
Unit-cell parameters (Å)	a = 128.0, c = 104.7	a = 128.8, c = 104.2		
Resolution (Å)	38.6–2.55 (2.64–2.55)	45.2–3.10 (3.27–3.10)	45.2–3.15 (3.32–3.15)	45.2–3.15 (3.32–3.15)
Reflections (observed/unique)	311493/28944	188785/16284	177981/15467	175132/15511
Completeness (%)	99.9 (99.9)	99.9 (99.9)	99.9 (99.9)	99.9 (99.9)
Redundancy	10.8 (11.1)	11.6 (11.8)	11.5 (11.8)	11.3 (11.6)
Averaged $I/\sigma(I)$	3.9 (2.0)	7.1 (2.2)	7.4 (2.5)	7.1 (2.4)
$R_{\rm meas}$† (%)	11.8 (38.3)	10.5 (37.1)	10.0 (32.0)	10.3 (32.3)
Phasing				
Resolution (Å)		39.5–3.2		
Mean FOM (overall/centric/acentric)		0.72/0.56/0.72		
Refinement				
Resolution (Å)	10.0–2.55			
$R/R_{\rm free}$ (%)	23.9/27.1			
No. of non-H atoms	4033			
Protein	4025			
MPD	8			
R.m.s.d. bond length (Å)	0.007			
R.m.s.d. bond angles (°)	1.30			
Ramachandran plot (%)				
Most favoured	85.9			
Additionally allowed	11.1			
Generously allowed	3.0			

† $R_{\rm meas} = \sum_h [m/(m-1)]^{1/2} \sum_j |\langle I\rangle_h - I_{h,j}| / \sum_h \sum_j I_{h,j}$, where $\langle I\rangle_h$ is the mean intensity of symmetry-equivalent reflections and m is the redundancy.

Number 4, 1994) was performed to improve the map quality. After construction of the molecular model for residues 59–588, side chains were generated automatically using *ARP/wARP* (Morris *et al.*, 2003). Several cycles of manual fitting with *O* combined with refinement by conjugate-gradient minimization and *B*-factor refinement with *CNS* (Brünger *et al.*, 1998) were carried out. The final refined model included 549 amino-acid residues and one MPD molecule. Residues 1–59 and 341–356 were unidentified in the electron-density map and thus molecular models for these segments are not present in the final model. As the side chains of residues 60–66 were also unidentified in the electron-density map, the main chains of these segments were constructed as polyglycine chains in the final model. The crystallographic *R* factor for reflections between 10.0 and 2.55 Å resolution was 23.9% with a free *R* factor of 27.1% based on a subset of 10% of the reflections. The statistics for phasing and refinement are also summarized in Table 1.

3. Results and discussion

Catalytic nucleotide-binding subunit A has a warped cylindrical structure with approximate dimensions of 55 × 55 × 100 Å (Fig. 1*b*). This subunit consists of four domains: domain I (N-terminal domain, residues 1–79, 110–116, 189–199), domain II [corresponds to the 'knob-like structure' observed in electron microscopy (Coskun, Radermacher *et al.*, 2004; Coskun, Chaban *et al.*, 2004), residues 117–188], domain III (nucleotide-binding domain, residues 80–99, 200–437) and domain IV (C-terminal domain, residues 438–588). Based on the amino-acid sequence alignment, the N-terminal disordered region (Met1–Val59) and Arg60–Leu76 are likely to correspond to the N-terminal crown region consisting of seven β-strands in the N-terminal domain of F_1-ATPase α and β subunits (Abrahams *et al.*, 1994). Loose crystal packing arising from the fact that the A subunit was not crystallized in complex with other subunits such as B and D as well as the high solvent content (61.2%) may have caused flexibility in most of the N-terminal domain and some parts of the nucleotide-binding domain and thus cause these regions to be disordered or to have high *B* factor. With the exception of domain II, which protrudes towards the outside of the subunit, the overall structure of subunit A closely resembles those of F_1-ATPase catalytic subunit β and non-catalytic subunit α, despite the low levels of sequence identity (about 20%, Fig. 1*c*).

In the major nucleotide-binding subunits α and β of F_1-ATPase and A and B of A_1/V_1-ATPase, two nucleotide-binding motifs, the Walker A motif (also called the nucleotide-binding P-loop, GPFGSGKT, residues 234–241) and the Walker B motif (RDMGYDDVALMAD, residues 320–331) are conserved (Walker *et al.*, 1982). All the residues essential for nucleotide binding and enzyme activity in the β subunit of the F_1-ATPase are strictly conserved in the primary sequence of the A subunit of both the A-ATPase and V-ATPase (Fig. 2*a*). No electron density corresponding to ATP, ADP or Mg^{2+} was observed in the nucleotide-binding site. The geometry of the active site is essentially the same as that of the F_1-ATPase β subunit. This conservation of the active-site geometry in the catalytic subunit A of A-ATPase strongly suggests that A-ATPase employs the same mechanism as F-ATPase.

The DELSEED sequence in the C-terminal domain of the bovine mitochondria F_1-ATPase β subunit, which moves and contacts the rotor γ subunit when the nucleotide fills the catalytic site (Hara *et al.*, 2000, 2001), is substituted for DALPERE (residues 482–488) in *Pho* A_1-ATPase A subunit (Fig. 2*b*). The bovine F_1-ATPase β DELSEED motif contains five acidic residues, whereas this region of *Pho* A_1 A subunit only contains three acidic residues. The negative charges in the F_1-ATPase β DELSEED motif do not play a direct role in torque generation, but its acidic property plays a role in the inhibitory effect by the intrinsic inhibitor, the F_1-ATPase ε

subunit (Hara *et al.*, 2000, 2001). The residues related to the interaction between the A and D/F subunits of A-ATPase have not been precisely determined, but the catalytic subunit A is likely to connect with the D and/or F subunit *via* this region. Further studies from both biochemical and structural perspectives are required to elucidate the role of this region in rotation catalysis of the A-ATPase.

Domain II, the novel domain which corresponds to the knob-like structure in the electron-microscopy projection of A_1A_0 ATP synthase (Coskun, Radermacher *et al.*, 2004; Coskun, Chaban *et al.*, 2004), was revealed between domain I (the N-terminal domain) and domain III (the nucleotide-binding domain). According to the model of subunit topology in the A_1A_0 complex proposed based on biochemical and structural data (Coskun, Radermacher *et al.*, 2004; Coskun, Chaban *et al.*, 2004), domain II protrudes toward the opposite side of the central rotor (Figs. 1*a* and 1*b*). Domain II is a peripheral domain including part of the NHR, which consists of about 90 amino acids and is highly conserved in A- and V-ATPase catalytic nucleotide-binding subunit A but is absent in the F-ATPase (Pro122–Pro210 of *Pho* A_1-ATPase A subunit; Fig. 2*c*). The structure-based sequence alignment provided detailed information on this region. The NHR previously assigned for the *Sce* V_1-ATPase A subunit does not fully correspond to domain II of the *Pho* A_1-ATPase A subunit. In fact, the C-terminal region of the previously assigned NHR, Met189–Pro210 of the *Pho* A_1-ATPase A subunit and Thr114–Ile136 of the bovine F_1-ATPase β subunit are homologous. Furthermore, Lys117–Ile121 of domain II of the *Pho* A_1-ATPase A subunit has no region homologous to F_1-ATPase β. The structure of the *Pho* A_1-ATPase A subunit suggests that we should modify the assignment of the NHR as Lys117–Lys188.

Domain II of *Pho* A_1-ATPase A subunit is a peculiar domain comprised of eight β-strands and is folded into a compact β-sandwich structure with internal twofold symmetry (Fig. 1*d*). The fold of this domain is very similar to the crystal structure of the biotinyl/lipoyl domain (Fig. 1*e*); for example, the biotinyl domain of acetyl-CoA carboxylase (PDB code 1bdo; Athappilly & Hendrickson, 1995) and the solution structures of the biotin carboxyl carrier domain of transcarboxylase (PDB code 1dcz; Reddy *et al.*, 2000), the lipoyl domain of pyruvate dehydrogenase (PDB codes 1iyu and 1qjo; Berg *et al.*, 1997; Jones *et al.*, 2000) and the lipoyl domain of 2-oxoglutarate dehydrogenase (PDB code 1ghj; Berg *et al.*, 1996). Despite the low levels of sequence identity (14–25%), superposition of the backbone of domain II onto these domains gives r.m.s.d. values of 0.9–1.4 Å. However, comparison between domain II of the *Pho* A_1-ATPase A subunit and the other protein domains indicates two differences: the absence of a Lys residue to be biotinylated or lipoylated and the topology of the strands. Firstly, the target of biotinylation or lipoylation is the Lys residue located in the loop between the fourth and fifth strands, whereas the residue at this position is Ser143 in the *Pho* A_1-ATPase A subunit. Secondly, although seven strands are compatible in both length and location, the last strand in domain II (residues 184–187) corresponds to the first strands in the other domains, resulting in a difference in topology.

The *Sce* V_1-ATPase A subunit NHR has been reported to bind directly to the V_0 domain and mutation in the NHR causes a change in proton-transport or ATPase activity and defective assembly of V-ATPase (Shao *et al.*, 2003; Shao & Forgac, 2004). The peripheral location of domain II of the *Pho* A_1-ATPase A subunit implies that this domain forms part of the peripheral stalk connecting the A_1 and A_0 domains. Taking the results of mutational analysis of the *Sce* NHR of the V_1-ATPAse A subunit into account (Shao *et al.*, 2003; Shao & Forgac, 2004), it is highly likely that domain II in the A subunit is related to the peripheral stalk common to the A- and V-ATPases. Although the detailed effects of mutation of the residues in domain II or the NHR have not been reported for A-ATPase, it is reasonable to suggest that this region plays an important role in A-ATPase as well as in V-ATPase based on the similarities in sequence, composition and topology of the subunits. Further investigations, including structural analysis of the A-ATPase complex or structural analysis of domain II in complex with the subunits forming part of the peripheral stalk of A-ATPase, will be necessary to determine whether this domain actually contributes to the peripheral stalk connecting A_1 and A_0.

We would like to thank M. Kawamoto of JASRI and S. Wakatsuki, M. Suzuki and N. Igarashi of KEK-PF for their assistance in the synchrotron experiments. This work was supported by a grant for the National Project on Protein Structural and Functional Analyses from the Ministry of Education, Culture, Sports, Science and Technology of Japan.

References

Abrahams, J. P. & Leslie, A. G. W. (1996). *Acta Cryst.* D**52**, 30–42.
Abrahams, J. P., Leslie, A. G. W., Lutter, R. & Walker, J. E. (1994). *Nature (London)*, **370**, 621–628.
Athappilly, F. K. & Hendrickson, W. A. (1995). *Structure*, **3**, 1407–1419.
Becher, B. & Muller, V. (1994). *J. Bacteriol.* **176**, 2543–2550.
Berg, A., Vervoort, J. & de Kok, A. (1996). *J. Mol. Biol.* **261**, 432–442.
Berg, A., Vervoort, J. & de Kok, A. (1997). *Eur. J. Biochem.* **244**, 352–360.
Bowman, E. J., Tenney, K. & Bowman, B. J. (1988). *J. Biol. Chem.* **263**, 13994–14001.
Brünger, A. T., Adams, P. D., Clore, G. M., DeLano, W. L., Gros, P., Grosse-Kunstleve, R. W., Jiang, J.-S., Kuszewski, J., Nilges, M., Pannu, N. S., Read, R. J., Rice, L. M., Simonson, T. & Warren, G. L. (1998). *Acta Cryst.* D**54**, 905–921.
Collaborative Computational Project, Number 4 (1994). *Acta Cryst.* D**50**, 760–763.
Coskun, U., Chaban, Y. L., Lingl, A., Muller, V., Keegstra, W., Boekema, E. J. & Gruber, G. (2004). *J. Biol. Chem.* **279**, 38644–38648.
Coskun, U., Radermacher, M., Muller, V., Ruiz, T. & Gruber, G. (2004). *J. Biol. Chem.* **279**, 22759–22764.
Cowtan, K. (1994). *Jnt CCP4/ESF–EACBM Newsl. Protein Crystallogr.* **31**, 34–38.
Dirmeier, R., Hauska, G. & Stetter, K. O. (2000). *FEBS Lett.* **467**, 101–104.
Forgac, M. (1999). *J. Biol. Chem.* **274**, 12951–12954.

Futai, M., Oka, T., Moriyama, Y. & Wada, Y. (1998). *J. Biochem.* **124**, 259–267.
Hara, K. Y., Kato-Yamada, Y., Kikuchi, Y., Hisabori, T. & Yoshida, M. (2001). *J. Biol. Chem.* **276**, 23969–23973.
Hara, K. Y., Noji, H., Bald, D., Yasuda, R., Kinosita, K. J. & Yoshida, M. (2000). *J. Biol. Chem.* **275**, 14260–14263.
Hirata, R., Ohsumi, Y., Nakano, A., Kawasaki, H., Suzuki, K. & Anraku, Y. (1990). *J. Biol. Chem.* **265**, 6726–6733.
Hochstein, L. I. (1992). *FEMS Microbiol. Lett.* **97**, 155–159.
Ihara, K. & Mukohata, Y. (1991). *Arch. Biochem. Biophys.* **286**, 111–116.
Jones, D. D., Stott, K. M., Howard, M. J. & Perham, R. N. (2000). *Biochemistry*, **39**, 8448–8459.
Jones, T. A., Zou, J. Y., Cowan, S. W. & Kjeldgaard, M. (1991). *Acta Cryst.* A**47**, 110–119.
La Fortelle, E. de & Bricogne, G. (1997). *Methods Enzymol.* **276**, 472–494.
Leyva, J. A., Bianchet, M. A. & Amzel, L. M. (2003). *Mol. Membr. Biol.* **20**, 27–33.
Maegawa, Y., Morita, H., Yao, M., Watanabe, N. & Tanaka, I. (2004). *Acta Cryst.* D**60**, 1484–1486.
Morris, R. J., Perrakis, A. & Lamzin, V. S. (2003). *Methods Enzymol.* **374**, 229–244.
Mukohata, Y. & Yoshida, M. (1987). *J. Biochem.* **101**, 311–318.
Puopolo, K., Kumamoto, C., Adachi, I. & Forgac, M. (1991). *J. Biol. Chem.* **266**, 24564–24572.
Reddy, D. V., Shenoy, B. C., Carey, P. R. & Sonnichsen, F. D. (2000). *Biochemistry*, **39**, 2509–2516.
Schafer, G. & Meyering-Vos, M. (1992). *Biochim. Biophys. Acta*, **1101**, 232–235.
Shao, E. & Forgac, M. (2004). *J. Biol. Chem.* **279**, 48663–48670.
Shao, E., Nishi, T., Kawasaki-Nishi, S. & Forgac, M. (2003). *J. Biol. Chem.* **278**, 12985–12991.
Terwilliger, T. (2004). *J. Synchrotron Rad.* **11**, 49–52.
Walker, J. E., Saraste, M., Runswick, M. J. & Gay, N. J. (1982). *EMBO J.* **1**, 945–951.
Wilms, R., Freiberg, C., Wegerle, E., Meier, I., Mayer, F. & Muller, V. (1996). *J. Biol. Chem.* **271**, 18843–18852.
Yasuda, R., Noji, H., Yoshida, M., Kinosita, K. J. & Itoh, H. (2001). *Nature (London)*, **410**, 898–904.
Zimniak, L., Dittrich, P., Gogarten, J. P., Kibak, H. & Taiz, L. (1988). *J. Biol. Chem.* **263**, 9102–9112.